*31st EPS Conference on Plasma Phys. London, 28 June - 2 July 2004 ECA Vol.**28G**, P-2.128 (2004)*

Preliminary EBW heating experiment on the TST-2 Spherical Tokamak

H.Kasahara[1], Y.Kamada[1], K.Sasaki[2], A.Ejiri[1], K.Hanada[3], M.Hasegawa[3], H.Hoshika[2], A.Iyomasa[3], K.Nakamura[3], H.Nozato[1], S.Ohara[4], K.N.Sato[3], S.Shiraiwa[1], Y.Takagi[4], Y.Takase[1], T.Yamada[4] and H.Zushi[3]

1. Graduate School of Frontier Sciences, Univ. Tokyo, Kashiwa 277-8561, Japan
2. Graduate School of Engineering Sciences, Kyushu Univ., Kasuga 816-8580, Japan
3. Research Institute for Applied Mechanics, Kyushu Univ., Kasuga 816-8580, Japan
4. Graduate School of Science, Univ. Tokyo, Tokyo 113-0033, Japan

Abstract

Tokyo Spherical Tokamak -2 (TST-2) was moved to Kyushu University to perform EBW heating experiments based on the X-B mode-conversion scenario. In order to control the density gradient in the mode conversion zone, the antennas were surrounded by a movable local limiter. Two types of antennas were used. Low reflectivity (< 25 %) was obtained in most cases. A possibility of electron heating is suggested by a small increase of the stored energy (by about 10%) and a large increase of soft X-ray emission ($h\nu$ > 1 keV) observed during RF injection.

1. Introduction

The electron Bernstein wave (EBW) is an attractive candidate for heating Spherical Tokamak (ST) plasmas. It is well known that the EBW can propagate in overdense plasmas (such as in an ST) and is strongly absorbed by electron cyclotron damping. However, a technique to excite the short wavelength EBW needs to be developed. In the X-B mode-conversion scenario proposed in Ref. 1, the externally launched X-mode is converted to the EBW. This conversion can be efficient if a suitable density gradient could be realized around the upper-hybrid resonance layer located near the plasma edge. In order to examine the feasibility of this scenario, the TST-2 spherical tokamak (R = 0.38 m, a = 0.25 m, B_t = 0.3 T, I_p = 0.14 MA) was temporarily moved from the University of Tokyo to Kyushu University (shown in Fig. 1), where high power microwave sources (200 kW @ 8.2 GHz) were available.

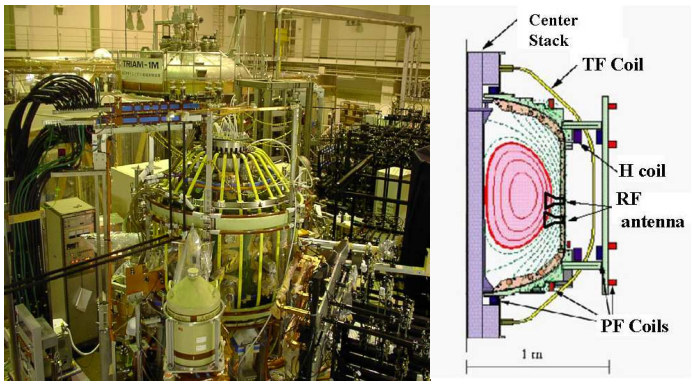

Fig. 1. (a) Photograph of TST-2 at Kyushu University (TST-2@K) and (b) its cross section.

2. Experimental setup

Figure 2 shows a schematic of the RF launcher installed on the low field side below the midplane of TST-2. Two types of launcher, each consisting of 8 waveguide antennas, were

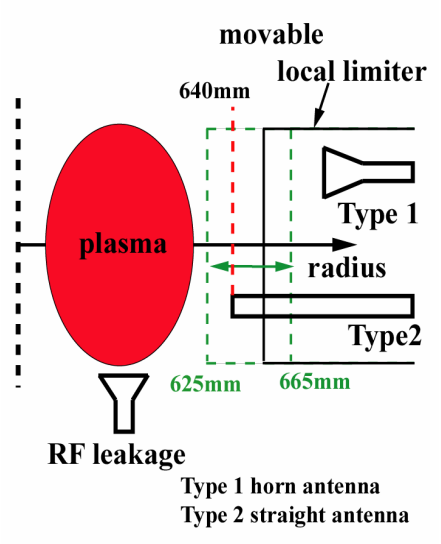

Fig.2. Schematic of two types of antennas relative to the plasma. The local limiter can be moved in the range shown.

used. The first type (Type 1) has horn antennas located at R = 755 mm. The second type (Type 2) has longer straight waveguides located at R = 640 mm. In order to control the density gradient in front of the antennas, these antennas were surrounded by a local limiter which was movable over the range R = 625 mm to 665mm. An RF leakage monitor was used as an indicator of RF power that was neither absorbed by the plasma nor reflected back to the launcher.

3. High power RF injection

Figure 3 shows a typical discharge in which nearly 100 kW of RF power was injected. The first RF pulse was used for preionization, during which the line integrated density $n_e l$ was low (< 1×10^{18} m^{-2}) and the RF leakage was large, suggesting poor absorption. In the second RF pulse, used for heating, the density was higher than the cut-off density ($n_e l > 4\times10^{18}$ m^{-2}) and the RF leakage became negligibly small. The level of the RF leakage power did not depend on either the local limiter position or the plasma current. Figure 4 shows the relationship between the local limiter position and the RF power reflectivity for the two types of launchers. Neither the plasma current nor the normalized RF leakage power were affected by the limiter position. The Type 1 launcher has lower reflectivities than the Type 2 launcher. A distinctively high reflectivity was observed when the local limiter was completely extracted so that the front face of the Type 2 antenna was in direct contact with the plasma. The highest reflectivity was observed in the discharge labeled 'high gas pressure'. In this discharge additional gas puff was applied to increase the edge density (and its gradient). As a result, the line integrated density $n_e l$ increased by 50%.

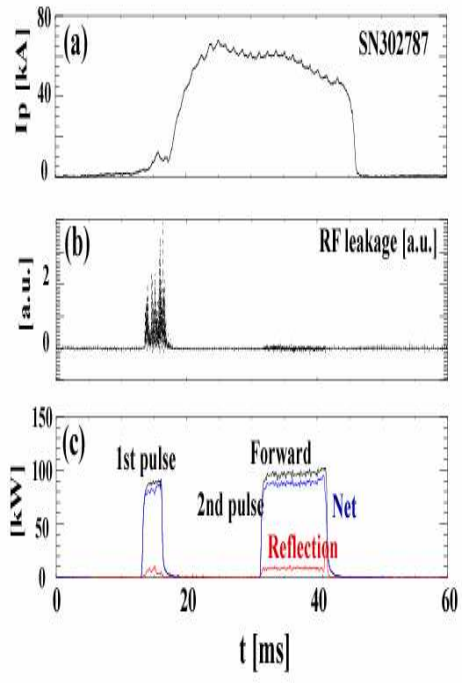

Fig.3. Time evolutions of (a) the plasma current I_p, (b) RF leakage and (c) RF powers (forward, reflected, and net).

4. Initial indication of EBW heating

In some discharges, a possible indication of EBW heating was observed. In Fig. 5,

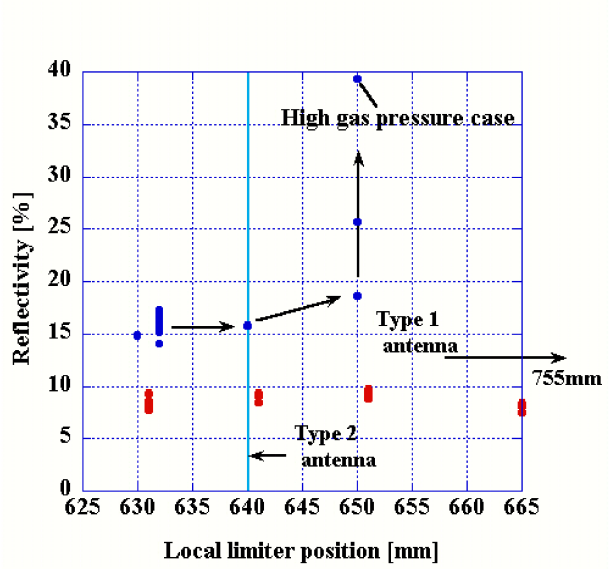

Fig.4. Dependence of the reflectivity on local limiter position. Large reflectivity is observed when the local limiter is pulled behind the Type2 (straight waveguide) launcher. Type 1 (horn) launcher is always located inside the local limiter.

representative parameters calculated by equilibrium reconstruction are shown. The plasma kinetic energy W_k increased from 150 to 170 J, and the total energy W_{tot} (kinetic plus poloidal magnetic) energy increased from 340 to 390 J, suggesting a possibility of current drive in addition to heating (note the increase) in I_p on the same time scale as the stored energy increase. The net injected RF power was 90 kW, whereas the ohmic input power was approximately 120 kW. If 50% of the injected RF power were assumed to be absorbed, an L-mode type energy confinement time scaling would predict a stored energy increase of 17%, which is not inconsistent with the observation. However, the absorbed power estimated from the break-in-slope analysis of the stored energy was only about 6 kW from $\Delta dW_k/dt$ (and 15 kW from $\Delta dW_{tot}/dt$). Time evolutions of $n_e l$, H_α, radiated power (measured by an AXUV detector), soft X-ray emission measured by SBD with Al (0.03–10 keV)or Be (1-10 keV) filter [SX (Al, Be)] are shown in Fig. 6. All these signals increased after RF turn-on. The rise time of SX (Be) was about 5 ms, which is similar to the rise time of the stored energy, suggesting that electron heating is responsible for the stored energy increase. Unfortunately, direct electron temperature measurement was not available during this experiment. Increases

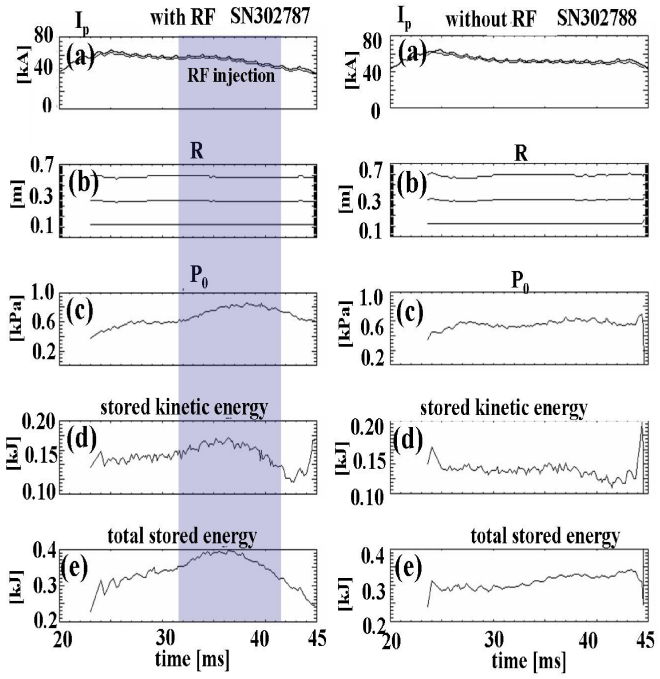

Fig.5. Time evolutions of (a) I_p, (b) plasma major radius and boundary positions , (c) central pressure, (d) kinetic energy, (e) kinetic plus poloidal magnetic energy. Left column with RF injection and right column without.

in $n_e l$, SX(Al), and P_{rad} were also observed. P_{rad} continued to increase after the stored energy has turned over, suggesting that the loss of heating is caused by increased radiation. A step-function like response of the H_α emission (rise time ~ 0.6 ms) indicates that some power is deposited directly in the plasma edge.

5. Conclusions and Summary

Successful RF power injection (net power ~ 100 kW) into an overdense plasma was achieved with low reflectivity. The low RF leakage power observed during the heating phase indicates that most of the injected power was absorbed by the plasma, either in the core or in the edge region. The reflectivity did not depend on the limiter position when the local limiter position was less than 640mm (*i.e.*, in front of the front face of the Type 2 antenna). The plasma kinetic energy and the total (kinetic plus poloidal magnetic) energy derived from equilibrium analysis increased during RF injection, as did $n_e l$, P_{rad} (AXUV), and SX emission. SX (Be) increased over the same time scale as the kinetic and total energies, suggesting that electron heating is responsible for the stored energy increase. Although the stored energy increase is not inconsistent with what is expected from an L-mode type energy confinement time scaling and approximately 50% absorption efficiency, the absorbed power estimated from the break-in-slope analysis was significantly lower. A more likely interpretation is that a large fraction of the mode-converted EBW power was lost before propagating into the plasma core. The observed stored energy increase of 20 J, expected from the absorbed power of 6 kW, may be partly due to the density dependence of energy confinement in ohmic plasmas.

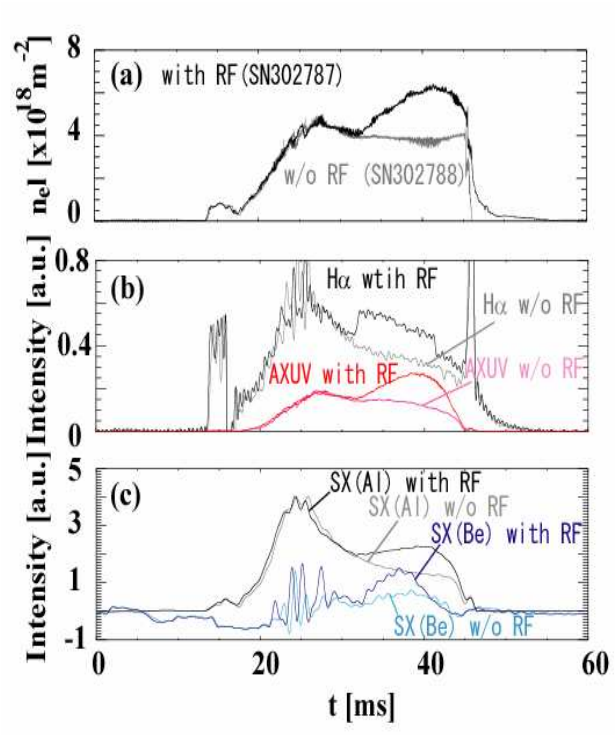

Fig.6. Time evolution of (a) $n_e l$, (b) H_α and P_{rad} (broadband radiation over the range 0.01 eV ~ 7 keV), (c) soft x-ray emission (Al: 30 eV ~ 10 keV, Be: 1 keV ~ 10 keV)

[1]A.K.Ram and S. D. Schultz, Phys. Plasmas **7**, 4084 (2000).